

See discussions, stats, and author profiles for this publication at: <https://www.researchgate.net/publication/282608517>

Multi-Phase Oscillatory Flow Strategy for in-situ Measurement and Screening of Partition Coefficients

ARTICLE *in* ANALYTICAL CHEMISTRY · OCTOBER 2015

Impact Factor: 5.64 · DOI: 10.1021/acs.analchem.5b03311

READS

27

3 AUTHORS, INCLUDING:



Milad Abolhasani

Massachusetts Institute of Technology

29 PUBLICATIONS 109 CITATIONS

SEE PROFILE

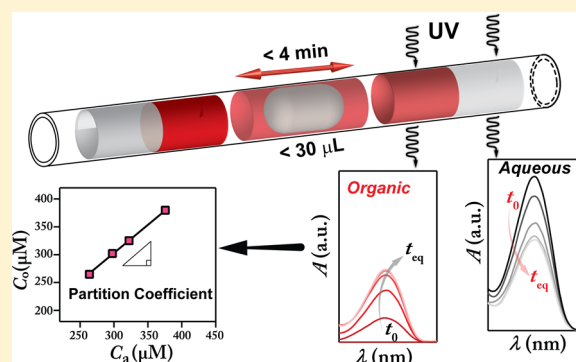
Multiphase Oscillatory Flow Strategy for *in Situ* Measurement and Screening of Partition Coefficients

Milad Abolhasani, Connor W. Coley, and Klavs F. Jensen*

Department of Chemical Engineering, Massachusetts Institute of Technology, 77 Massachusetts Avenue, 66-342, Cambridge, Massachusetts 02139, United States

W Web-Enhanced Feature S Supporting Information

ABSTRACT: Taking advantage of the difference between the surface energies of aqueous and organic solvents on a Teflon substrate, a fully automated small-scale strategy is developed on the basis of gas-driven oscillatory motion of a biphasic slug for high-throughput *in situ* measurement and screening of partition coefficients of organic substances between aqueous and organic phases. The developed oscillatory flow strategy enables single partition coefficient data point measurement within 8 min (including the sample preparation time) which is 360 times faster than the conventional “shake-flask” method, while using less than a 30 μL volume of the two phases and 9 nmol of the target organic substance. The developed multiphase strategy is validated using a conventional shake-flask technique. Finally, the developed strategy is extended to include automated screening of partition coefficients at physiological temperature.



A partition coefficient (sometimes known as distribution coefficient) describes the hydrophilicity or hydrophobicity of a compound between two immiscible phases and has a wide range of applications in the pharmaceutical industry (e.g., pharmacokinetics and pharmacodynamics)^{1–3} and environmental sciences (i.e., groundwater contamination).^{4–6} Conventionally, a partition coefficient is measured in batch scale using the “shake-flask” method (using UV spectroscopy or HPLC for analysis), shown in Figure 1a.^{7–9} However, the large diffusion length scales associated with batch techniques necessitate the

creation of microemulsions to promote mass transfer; in turn, the presence of these emulsions increases the time required for separation of the two immiscible phases after equilibrium, making the batch scale technique a time- and labor-intensive process. Moreover, the manual batch scale technique is challenging to apply to partition coefficient measurements at physiologically relevant temperatures (i.e., 37 °C).

Over the past decade, continuous microscale multiphase strategies, owing to their enhanced heat and mass transfer characteristics,^{10,11} have been developed as an alternative route to batch scale multiphase processes such as liquid–liquid extraction^{12–15} and screening of gas dissolution and solubility.^{16–21} Recently, multiphase microfluidics approaches have also been applied for measurement of partition coefficient between two immiscible phases.^{22–25} These microscale strategies have (i) used a microfluidic device as an efficient mixing method for “fast” equilibrium times and downstream phase separation and collection of each phase for manual measurements,^{24,25} (ii) utilized fluorescence microscopy for measurements of the extraction of a fluorescent molecule from one phase to another,²² or (iii) used gravity and as the method of shaking (mixing) and phase separation.²³ Although these microscale strategies have shown promising alternatives to the batch scale shake-flask method, the phase separation process, downstream collection, and manual characterization of each phase makes the measurement a semibatch process. In addition,

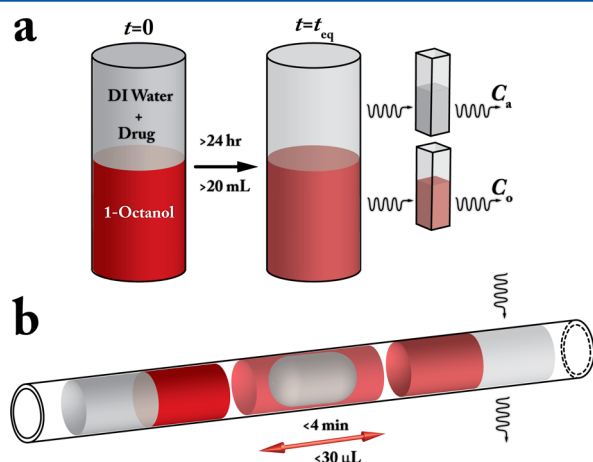


Figure 1. Schematic illustration of (a) the batch scale “shake-flask” and (b) the small scale oscillatory flow techniques for measurement of the partition coefficient.

Received: August 28, 2015

Accepted: October 5, 2015

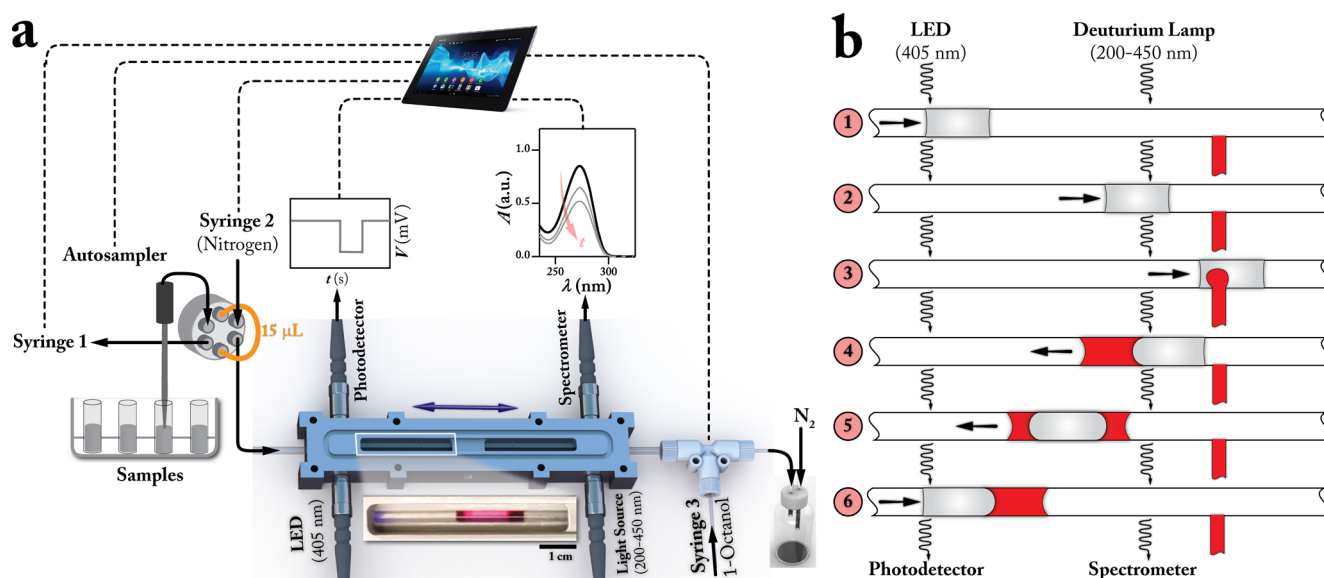


Figure 2. (a) Schematic of the automated multiphase oscillatory flow platform for *in situ* measurement of partition coefficient. Syringe 1: withdraws liquid from the sample vials and delivers into the sample loop. Syringe 2: delivers carrier phase, prefilled with 10 psig nitrogen. Syringe 3: injects the organic phase (1-octanol) into the aqueous phase (DI water) containing the organic substance. (b) Illustration of different steps associated with injection of the organic phase into the aqueous phase and the subsequent oscillatory motion of the biphasic slug within the tubular reactor.

fluorescence microscopy²² limits the applicability of the measurement technique to fluorophore molecules. These limitations, along with the constantly increasing need for rapid and accurate partition coefficient measurement of organic substances between two immiscible phases, necessitate the development of a fully automated small-scale process for *in situ* measurement and screening of the partition coefficient at the desired temperature.

Our group has recently developed a novel three-phase small-scale strategy for enhancing the mass transfer characteristics of continuous multiphase approaches for in-flow screening of biphasic catalytic reactions,²⁶ based on an oscillatory motion of a droplet in a confined space.^{27–29} Building on this idea, herein we report the design and development of a fully automated strategy for *in situ* measurement of partition coefficients of drug molecules within 8 min (including the sample preparation time), while using less than a 15 µL volume each of the aqueous and organic phases and only 9 nmol of the organic substance (Figure 1b).

Utilizing the difference between the surface energies of aqueous and organic phases on a Teflon substrate enables time-resolved *in situ* spectral characterization of the organic substance within each phase without additional phase separation. In addition, the use of gas (nitrogen) as the carrier phase facilitates the oscillatory motion thereby removing the residence time limitation associated with continuous multiphase microscale platforms.²⁷ More importantly, the oscillatory motion of the biphasic slug enables single-point spectral characterization of the biphasic slug during the transfer of the organic substance from the aqueous to the organic phase, as well as at the equilibrium state. While traditional techniques (with distinct mixing and measurement stages) often require assumptions about equilibration time, the system described herein can detect equilibration both quantitatively and automatically.

EXPERIMENTAL SECTION

DI water (cell culture grade water tested to USP sterile water for injection specifications, Mediatech, Inc., USA) and 1-octanol (ACS reagent, ≥99%, Sigma-Aldrich Co., USA) are used as the representative aqueous and organic phases within the human body. Caffeine (Pharmagrade, Sigma-Aldrich Co., USA) and acetaminophen (United States Pharmacopeia, Sigma-Aldrich Co., USA) are used as two drug species representative of hydrophilic and hydrophobic drugs at room temperature, respectively. DI water and 1-octanol were stored together to ensure thorough cosaturation before sample preparations.

The automated multiphase oscillatory platform, shown in Figure 2a, consists of a 12 cm long fluorinated ethylene propylene (FEP, 0.125 in. O.D., 0.0625 in. I.D., McMaster Carr, USA) tubing embedded within a custom-machined aluminum chuck (Proto Laboratories Inc., USA). A fiber-coupled LED (405 nm, Thorlabs Inc., USA) aligned with a fiber-coupled photodetector (Si switchable gain detector, Thorlabs Inc., USA) is integrated at the left side of the aluminum chuck for optical detection of the biphasic slug and reversal of the flow direction. The measured voltage from the photodetector was read directly in a custom LabVIEW code through an analog voltage I/O device (USB 6009, National Instruments, USA) to detect the gas–liquid boundary at the leading edge of the slug. A fiber-coupled UV–vis light source (DH-2000-BAL, Ocean Optics Inc., USA) aligned with a fiber-coupled miniature spectrometer (HR 2000+, Ocean Optics Inc., USA) is integrated at the right side of the aluminum chuck for (a) automatic acquisition of the absorption spectra within the aqueous and the organic phases and (b) reversal of the flow direction for the oscillatory motion of the biphasic slug. Extreme solarization resistant fibers (QP600-1-XSR, 180–800 nm, single-mode premium grade, Ocean Optics Inc., USA) are used for long-term reliable UV spectral measurements. A PID temperature controller (CN 9300, Omega Engineering Inc., USA) in combination with two cartridge heaters (Omega Engineering Inc., USA) embedded in each side of the

aluminum chuck and a K-type thermocouple (Omega Engineering Inc., USA) are used for real-time temperature control of the Teflon tube. A computer-controlled liquid handler (GX-241, Gilson Inc., USA) in combination with a syringe pump (GX syringe pump, Gilson Inc., USA) and an injection module (6-port injection valve) equipped with a 15 μL sample loop is used for automated sample preparation and fluid delivery into the experimental platform. The volume of the aqueous phase, V_{A} , is defined by the volume of the sample loop inserted into the injection module. For each organic compound, three samples including, DI water (cosaturated with 1-octanol), DI water containing a known concentration of the organic substance (e.g., caffeine and acetaminophen), and 1-octanol containing a known concentration of the organic compound were loaded in a vial rack. A computer-controlled syringe pump (PHD Ultra, Harvard Apparatus, USA) prefilled with nitrogen (10 psig) is used for delivery of the prepared slug from the sample loop to the oscillatory zone of the Teflon tube as well as for oscillatory motion of the biphasic slug after addition of the organic phase into the aqueous slug. Another computer-controlled syringe pump (PHD 2000, Harvard Apparatus, USA), equipped with a 250 μL glass syringe (SGE gastight syringes with luer lock, Sigma-Aldrich, USA) is used for synchronized injection of the desired volume of 1-octanol (cosaturated with DI water), V_{O} , into the preformed aqueous slug at a T-junction (PEEK, 0.02 in. through hole, IDEX Health and Science, USA) placed after the aluminum chuck. A pressurized reservoir at the outlet ensures the carrier phase (nitrogen) within the course of the partition coefficient experiment stays at the prefilled pressure (10 psig). For more details on the experimental setup and the automated oscillatory motion of the biphasic slug, including the overall LabVIEW logic used to control the process, see [Supporting Information Section S1](#).

Figure 2b illustrates different steps involved during the partition coefficient measurement experiment within the automated gas-driven oscillatory flow setup. (1) A 15 μL aqueous slug (without the organic substance) is automatically prepared by the liquid handler, injected into the Teflon reactor, and moved toward the spectral measurement point. The intensity spectrum of this aqueous slug is used as the reference for the real-time absorbance measurement of the aqueous phase during the oscillatory motion. Next, another 15 μL aqueous slug containing a known concentration of the organic compound is delivered into the sample loop and moved toward the first spectral measurement point. (2) The initial absorption spectrum of the organic substance within DI water is acquired with an integration time, t_{i} , of 20 ms and averaged over 40 spectra. This absorbance value is used to verify the initial concentration of the organic substance within the aqueous phase, $C_{\text{a}}(t_0)$. (3) Upon reaching the T-junction after the aluminum chuck, the carrier syringe pump is stopped and the organic phase (1-octanol) is injected into the aqueous slug containing the organic substance. (4) The flow direction of the carrier syringe is reversed (i.e., from infuse to withdraw), and the biphasic slug is moved back toward the measurement point. The absorption spectra of the aqueous and the organic phases are acquired (20 ms integration time, averaged over 20 spectra). After entering the oscillation zone of the Teflon tube, the carrier flow rate for the oscillatory stage of the experiment, Q_{osc} , is set to 600 $\mu\text{L}/\text{min}$ (see snapshot (i) of Figure 3). Details for selection of the appropriate oscillation flow velocity is explained elsewhere.²⁶ (5) Owing to the higher surface



Figure 3. Bright-field snapshot time-series of the oscillatory motion of a biphasic slug (DI water, 15 μL , and 1-octanol, 10 μL) along the Teflon tube embedded within the aluminum chuck (see [Movie M1](#)). The organic phase (1-octanol) is labeled with Sudan red for better visualization. Dashed lines in frames 5 and 10 highlight the aqueous phase. (i) UV absorption spectra of both phases are recorded, and the flow direction is reversed. (ii) Change in the measured voltage of the fiber-coupled photodetector results in the detection of the biphasic slug, and the flow direction is reversed. (iii) Completely separated aqueous and organic phases within the biphasic slug enter the UV spectral measurement point.

tension of the aqueous phase compared to the organic phase and the relatively low interfacial tension at the interface between the two immiscible phases as well as the lower surface energy of the aqueous phase compared to the organic phase on the FEP tube, the aqueous phase moves more freely along the flow direction in comparison to the organic phase. The more facile motion of the aqueous phase in comparison to the organic phase on the Teflon tube wall results in the displacement of the aqueous phase from the back to the front of the biphasic slug through the organic phase, resulting in the complete engulfment of the aqueous phase within the organic phase while moving from the right to the left of the oscillation zone of the setup.^{26,30,31} (6) After moving through the organic phase and leading the biphasic slug, the aqueous segment of the biphasic slug reaches the fiber-coupled LED aligned with the fiber-coupled photodetector integrated at the left side of the aluminum chuck. The presence of the aqueous phase in front of the light emitted from the fiber-coupled LED changes the amount of light transferred through the tube wall and absorbed by the fiber-coupled photodetector, thereby changing the measured voltage with the data acquisition toolbox. This change in the measured voltage of the photodetector is used as the threshold criterion for detection of the biphasic slug at the left side of the oscillation zone. After detecting the leading edge of the biphasic slug through the change in the measured voltage of the photodetector, the flow direction of the carrier phase syringe pump is automatically reversed (i.e., from withdraw to infuse), and the biphasic slug is pushed back toward the spectral measurement point integrated

at the right end of the aluminum chuck (see snapshot (ii) of Figure 3). Next, owing to the same physical phenomena explained in stage (5), during the motion of the biphasic slug from the left to the right end of the aluminum chuck, the aqueous segment of the biphasic slug moves through the organic phase and leads the biphasic slug before reaching the spectral measurement point (see snapshot (iii) of Figure 3). The complete separation of the aqueous and organic phases before passing through the spectral measurement point enables *in situ* acquisition of the absorption spectrum of the organic substance within both the aqueous and organic phases without the need for any phase separation strategy such as in-line membrane²⁵- or gravity²⁴-based phase separation techniques.

The number of oscillation cycles, N , is defined such that the absorbance at the target wavelength(s) reaches a constant value, indicating mass-transfer equilibrium. The concentration of the organic substance in the aqueous phase, C_a , and the organic phase, C_o , at each instant of time, t , and the defined temperature, T , is measured using an absorbance calibration curve at the target wavelength(s), λ , obtained through an automated serial dilution of the aqueous and organic phase stock solutions containing a known concentration of the organic compound within the liquid handler:

$$C_a(T, t) = j_a A_a(\lambda, T, t) \quad (1)$$

$$C_o(T, t) = j_o A_o(\lambda, T, t) \quad (2)$$

where j_a and j_o are the calibration constants and A_a and A_o are the absorbance values at the target wavelength, within the aqueous and the organic phases, respectively. Employing eqs 1 and 2, the partition coefficient of the organic substance between the two immiscible phases is calculated using the experimentally measured absorbance values of the aqueous and the organic phases at the equilibrium:

$$P(T) = \frac{C_o(T, t_{eq})}{C_a(T, t_{eq})} = \frac{j_o A_o(\lambda, T, t_{eq})}{j_a A_a(\lambda, T, t_{eq})} \quad (3)$$

After each partition coefficient measurement experiment, three wash slugs (DI water cosaturated with 1-octanol) were introduced into the FEP tubing through the sample loop, using the automated liquid handler to eliminate any carry-over between two consecutive slugs.

The utilization of a fiber-coupled deuterium light source and a miniature spectrometer for the characterization of the organic substance concentration, instead of a LED and a photodetector, enables the absorbance measurements over a wider range of wavelengths from 200 to 450 nm rather than only one specific wavelength associated with the LED source. This not only extends the range of measurable organic substances with the multiphase oscillatory platform but also allows for the use of principal component analysis (PCA) or principal component regression (PCR) for quantification when high precision is required. The partition coefficient calculation (eq 3) is changed according to the chosen regression model.

RESULTS AND DISCUSSION

In order to ensure a linear relationship between the measured absorbance values and the concentrations of the organic substance (i.e., Beer–Lambert law) within the aqueous and the organic phases, we performed an automated serial dilution of the prepared stock solutions of the aqueous and the organic phases with known concentrations of the target organic

compound, using the automated liquid handler. The stock solutions were sequentially aspirated, stirred inside the liquid handler needle, and diluted to 1:2, 1:3, 1:4, 1:5, and 1:6 volume ratios with the corresponding pure solvent. The resulting slug was injected into the sample loop and moved toward the spectral measurement point. The measured absorbance values at the target wavelength exhibited excellent linearity with concentrations of the organic compound (see Supporting Information Section S2).

In the next step, we characterized the mass transfer of a hydrophilic drug (i.e., caffeine) between cosaturated DI water and 1-octanol. Figure 4a shows the time-evolution of the *in situ*

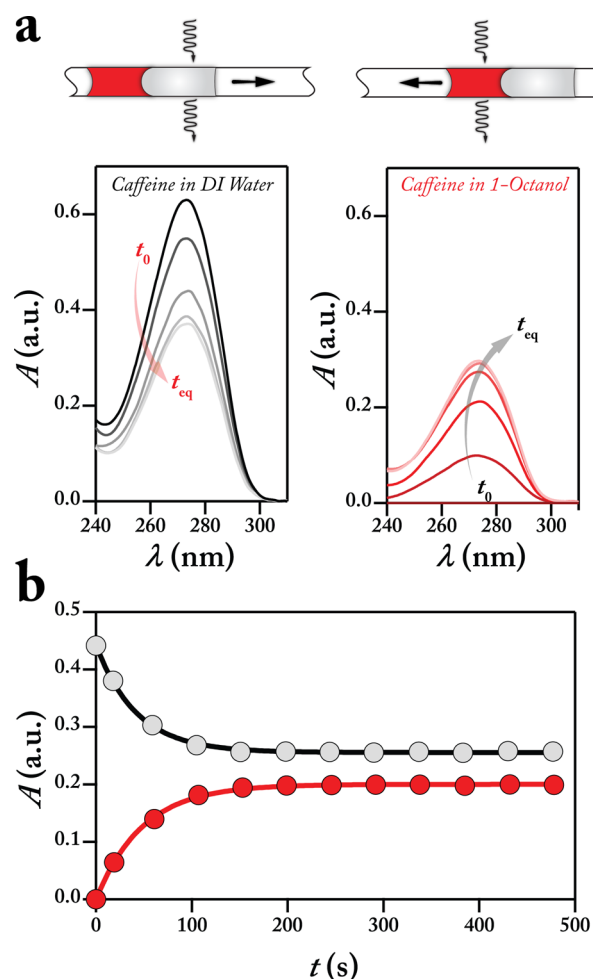


Figure 4. (a) Absorption spectra time-evolution of caffeine within the aqueous (DI water) and the organic (1-octanol) phases. (b) Temporal evolution of the caffeine absorbance at A_{273} – A_{290} within (gray ●) the aqueous and (red ●) the organic phases: $C_a(t_0) = 507 \mu\text{M}$, $C_o(t_0) = 484 \mu\text{M}$, $V_A = 15 \mu\text{L}$, $V_O = 12.5 \mu\text{L}$, $Q_{osc} = 600 \mu\text{L}/\text{min}$, $t_1 = 20 \text{ ms}$, $N = 10$, and $T = 23^\circ\text{C}$.

obtained UV absorption spectra of caffeine within the aqueous and the organic phases. Employing a custom-developed MATLAB script, the absorbance of caffeine within the aqueous and the organic phases at a defined wavelength was automatically extracted from each acquired absorption spectrum (Figure 4a) and plotted in Figure 4b for different oscillation cycles (i.e., times). In order to obtain the standard deviation for the measured value of the partition coefficient at each temperature, we conducted the multiphase oscillatory

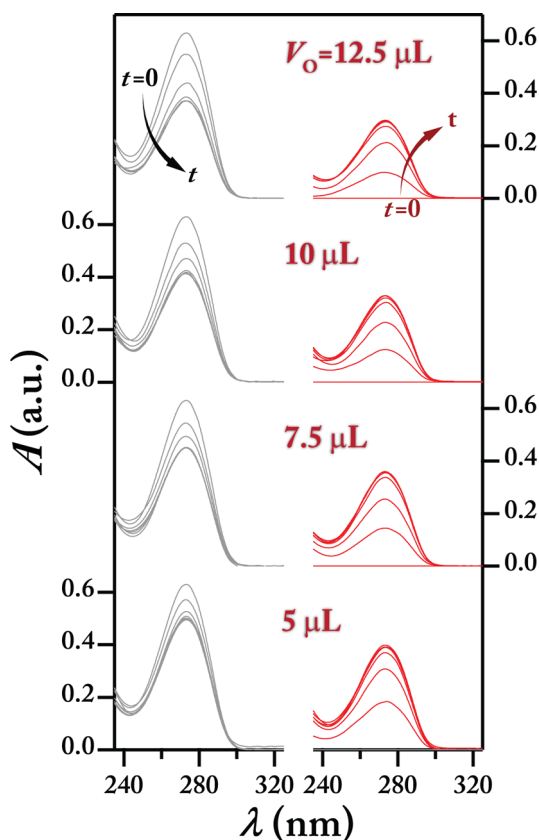


Figure 5. *In situ* time-evolution of absorption spectra of caffeine in (gray —) the aqueous and (red —) the organic phase for different aqueous-to-organic volume ratios; $C_a(t_0) = 507 \mu\text{M}$, $C_o(t_0) = 484 \mu\text{M}$, $V_A = 15 \mu\text{L}$, $Q_{\text{osc}} = 600 \mu\text{L}/\text{min}$, $t_1 = 20 \text{ ms}$, $N = 10$, and $T = 23^\circ\text{C}$.

experiment at four different aqueous-to-organic volume ratios, R_{AO} . The UV spectral evolution of caffeine within DI water and 1-octanol for different values of R_{AO} is shown in Figure 5. As shown in Figure 5, by decreasing the volume of the organic phase, the equilibrium absorbance values of caffeine in the aqueous and the organic phases increase (i.e., the concentration of caffeine in both phases increase), while the total number of moles of caffeine was maintained within all biphasic slugs. The *in situ* obtained temporal evolution of caffeine absorbance within DI water and 1-octanol for different values of R_{AO} is shown in Figure 6a. As shown in Figure 6a, caffeine absorbance values within the aqueous and the organic phases reach equilibrium in less than 4 min (shown with the dashed line in Figure 6a). It should also be noted that the experimentally measured equilibrium time (shown in Figure 6a) is ~ 70 times shorter than the one-dimensional characteristic diffusion time of caffeine within a 2.5 mm ($\sim 5 \mu\text{L}$) water slug and estimated diffusivity of $4.9 \times 10^{-10} \text{ m}^2/\text{s}$ at $T = 23^\circ\text{C}$ (using Stokes–Einstein equation and caffeine hydrodynamic diameter of $\sim 1 \text{ nm}$);³² convection effects caused by the oscillatory motion of the biphasic slug are necessary to achieve equilibrium in such a short time.

Utilizing the previously obtained calibration coefficients for each phase, the measured absorbance values at the equilibrium state were used to calculate the corresponding caffeine concentrations in the aqueous and the organic phases. The equilibrium concentrations of caffeine within the aqueous and the organic phases at different values of R_{AO} and two different

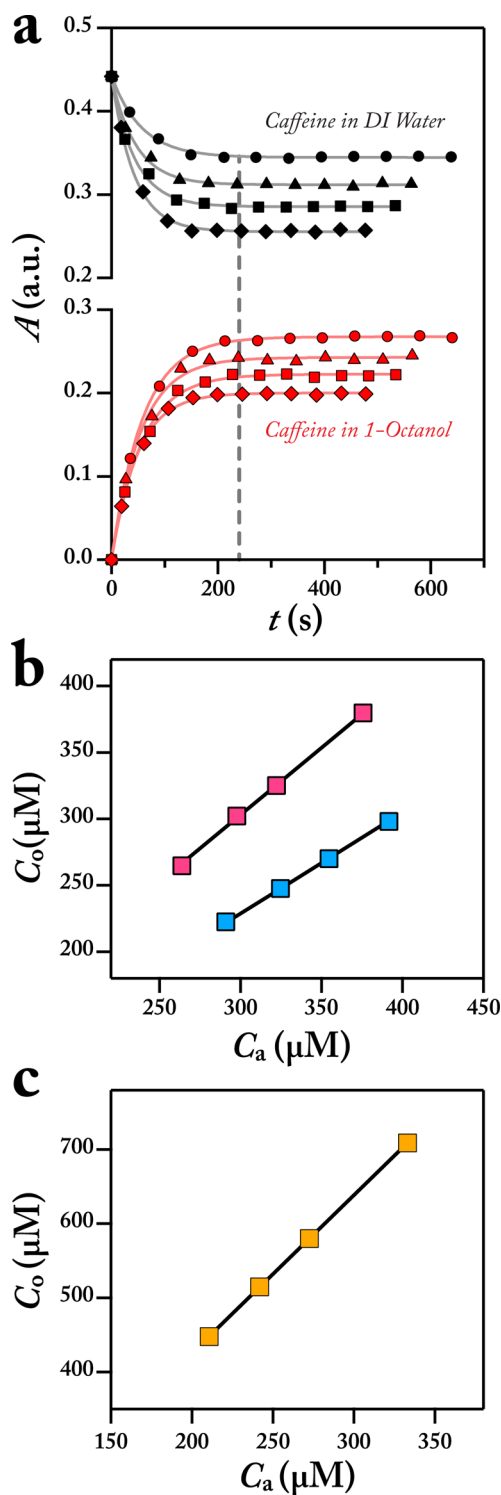


Figure 6. (a) *In situ* obtained caffeine absorbance at A_{273} – A_{290} within the aqueous, A, and the organic, O, phases for different aqueous/organic volume ratios: (A black ●, O red ●) $R_{\text{AO}} = 3$, (A black ▲, O red ▲) $R_{\text{AO}} = 2$, (A black ■, O red ■) $R_{\text{AO}} = 1.5$, and (A black ◆, O red ◆) $R_{\text{AO}} = 1.2$; $C_a(t_0) = 507 \mu\text{M}$, $C_o(t_0) = 484 \mu\text{M}$; $V_A = 15 \mu\text{L}$, $Q_{\text{osc}} = 600 \mu\text{L}/\text{min}$, $t_1 = 20 \text{ ms}$, $N = 10$, and $T = 23^\circ\text{C}$. (b) Equilibrium concentrations of caffeine in the aqueous and the organic phase for different volume ratios at (a) (blue ■) $T = 23^\circ\text{C}$ and (pink ■) $T = 37^\circ\text{C}$. (c) Equilibrium concentrations of acetaminophen in the aqueous and the organic phases at A_{265} – A_{290} for different values of R_{AO} and $C_a(t_0) = 602 \mu\text{M}$, $C_o(t_0) = 535 \mu\text{M}$, $V_A = 15 \mu\text{L}$, $Q_{\text{osc}} = 600 \mu\text{L}/\text{min}$, $t_1 = 20 \text{ ms}$, $N = 10$, and $T = 23^\circ\text{C}$.

temperatures (room temperature, 23 °C, and the physiological human body temperature, 37 °C) are shown in Figure 6b. Using these equilibrium concentration values, the partition coefficient values, P , for caffeine at 23 and 37 °C are calculated to be 0.76 ± 0.0015 ($\log P = -0.118$) and 1.001 ± 0.0038 ($\log P = 0.004$), respectively. The small standard deviation of the measured values of caffeine partition coefficients using the automated multiphase oscillatory flow demonstrates the great reproducibility of the developed strategy.

In order to validate the measured values of P using the oscillatory flow strategy, we measured the partition coefficient of caffeine using the conventional shake-flask technique using different volume ratios of DI water and 1-octanol (1:1, 1.5:1, 4:1, and 0.66:1) and a cuvette-based UV spectroscopy technique (See Supporting Information Section S3, for more details of the batch scale partition coefficient measurements).

The value of caffeine partition coefficient using the batch scale technique at 23 °C was measured to be 0.77 ± 0.023 , in good agreement with the experimentally measured value of P using the developed oscillatory flow strategy. This result further demonstrates the accuracy of the developed oscillatory flow-based technique.

Furthermore, in comparison with the manual batch scale technique which requires more than 20 mL of each phase as well as long waiting times associated with mixing and further phase separation of the two immiscible phases (>24 h) for sampling and cuvette-based UV absorption measurements, the developed oscillatory multiphase strategy allows for rapid automated measurement and screening of P for different organic compounds in less than 8 min, while using less than 30 μL of both phases. As can be seen in Figure 6b, there is a statistically significant difference between the experimentally measured values of P at room temperature compared to the physiological temperature. This result highlights the need to screen P for different drug molecules at the physiological human body temperature, rather than ambient temperatures, which is substantially more difficult when using traditional shake-flask methods. In the next step, in order to further exploit the developed oscillatory flow strategy for high-throughput measurements of partition coefficient for different organic substances, we chose to study the partition coefficient of a hydrophobic drug molecule (acetaminophen). Figure 6c shows the experimentally measured concentrations of acetaminophen within the aqueous and the organic phases at the equilibrium condition and room temperature, 23 °C (See Supporting Information Section S4). Using the equilibrium concentration values of acetaminophen in DI water and 1-octanol, shown in Figure 6c, we calculated the partition coefficient of acetaminophen to be 2.128 ± 0.001 ($\log P = 0.328$) which is in a good agreement with the reported literature value of 2.13 ($\log P = 0.33$).^{25,33}

The primary source of error in partition coefficients measured using the automated flow strategy is the accuracy of syringe pumps used for droplet preparation and injection. Volume errors are reported as not exceeding 0.1 μL for the particular pumps and syringes selected for this study. Further, any volume errors will offset each other over the course of repeated trials due to the nature of syringe pump stepper motors. This is consistent with the observed high reproducibility.

Although equilibrium concentrations shown above are in excess of 100 μM , this strategy can similarly be applied to substrates at lower concentrations. The use of UV spectroscopy

as the fundamental analytical technique enables partition coefficient screening of any solute provided an absorbance spectrum can be detected (i.e., above 0.05 a.u.). To improve measurements for solutes with low solubility or UV absorbance, spectral signal-to-noise ratios can be increased by (a) upgrading the fiber-coupled spectrometer or (b) increasing total sampling time at each measurement cycle.

CONCLUSIONS

In conclusion, we designed and developed a fully automated small-scale strategy for high-throughput *in situ* measurement and screening of partition coefficient of organic substances between aqueous and organic phases at different temperatures. The developed multiphase oscillatory flow strategy enabled near-simultaneous measurements of absorption spectra of both aqueous and organic phases without the need for adapting any in-line phase separation techniques. A single partition coefficient value at a defined temperature was measured in less than 8 min (less than 1% of the time required by batch scale techniques), while using a biphasic slug with a total volume of less than 30 μL . The applicability of the developed strategy was demonstrated for both hydrophilic (caffeine) and hydrophobic (acetaminophen) drug molecules. The developed multiphase strategy could further be utilized for *in situ* screening of liquid–liquid extraction as well as partition coefficient screening of groundwater organic contaminants.

ASSOCIATED CONTENT

Supporting Information

The Supporting Information is available free of charge on the ACS Publications website at DOI: 10.1021/acs.analchem.5b03311.

Details of the automated liquid handling, the oscillatory motion of the biphasic slug, and absorption spectra evolution of acetaminophen. (PDF)

Web-Enhanced Feature

A movie showing the room temperature oscillatory motion of a biphasic slug (15 μL of DI water, 10 μL of 1-octanol labeled with Sudan red) within an FEP tube embedded inside the aluminum chuck with an oscillatory flow rate of 550 $\mu\text{L}/\text{min}$ in MPG format is available in the online version of the paper.

AUTHOR INFORMATION

Corresponding Author

*E-mail: kfjensen@mit.edu. Homepage: <http://web.mit.edu/jensenlab>.

Author Contributions

The manuscript was written through contributions of all authors. All authors have given approval to the final version of the manuscript.

Notes

The authors declare no competing financial interest.

ACKNOWLEDGMENTS

We thank the Novartis Center for Continuous Manufacturing for funding this research. M.A. gratefully acknowledges financial support from the NSERC Postdoctoral Fellowship. C.W.C. thanks the National Science Foundation Graduate Research Fellowship Program for support under Grant No. 1122374.

■ REFERENCES

- (1) Lipinski, C. A.; Lombardo, F.; Dominy, B. W.; Feeney, P. J. *Adv. Drug Delivery Rev.* **2012**, *64*, 4–17.
- (2) Wells, J. I. *Pharmaceutical preformulation: The physicochemical properties of drug substances*; Halsted Press: New York, 1988.
- (3) Baker, R. W.; Lonsdale, H. In *Controlled release of biologically active agents*; Springer: New York, 1974; pp 15–71.
- (4) Holm, J. V.; Ruegge, K.; Bjerg, P. L.; Christensen, T. H. *Environ. Sci. Technol.* **1995**, *29*, 1415–1420.
- (5) Jelic, A.; Gros, M.; Ginebreda, A.; Cespedes-Sánchez, R.; Ventura, F.; Petrovic, M.; Barcelo, D. *Water Res.* **2011**, *45*, 1165–1176.
- (6) Radjenović, J.; Petrović, M.; Barceló, D. *Water Res.* **2009**, *43*, 831–841.
- (7) Dearden, J. C.; Bresnen, G. M. *Quant. Struct.-Act. Relat.* **1988**, *7*, 133–144.
- (8) De Bruijn, J.; Busser, F.; Seinen, W.; Hermens, J. *Environ. Toxicol. Chem.* **1989**, *8*, 499–512.
- (9) Harnisch, M.; Möckel, H. J.; Schulze, G. J. *Chromatogr. A* **1983**, *282*, 315–332.
- (10) Song, H.; Chen, D. L.; Ismagilov, R. F. *Angew. Chem., Int. Ed.* **2006**, *45*, 7336–7356.
- (11) Teh, S.-Y.; Lin, R.; Hung, L.-H.; Lee, A. P. *Lab Chip* **2008**, *8*, 198–220.
- (12) Mary, P.; Studer, V.; Tabeling, P. *Anal. Chem.* **2008**, *80*, 2680–2687.
- (13) Lestari, G.; Abolhasani, M.; Bennett, D.; Chase, P.; Günther, A.; Kumacheva, E. *J. Am. Chem. Soc.* **2014**, *136*, 11972–11979.
- (14) Kralj, J. G.; Sahoo, H. R.; Jensen, K. F. *Lab Chip* **2007**, *7*, 256–263.
- (15) Kralj, J. G.; Schmidt, M. A.; Jensen, K. F. *Lab Chip* **2005**, *5*, 531–535.
- (16) Abolhasani, M.; Singh, M.; Kumacheva, E.; Gunther, A. *Lab Chip* **2012**, *12*, 1611–1618.
- (17) Abolhasani, M.; Singh, M.; Kumacheva, E.; Gunther, A. *Lab Chip* **2012**, *12*, 4787–4795.
- (18) Lefortier, S. G. R.; Hamersma, P. J.; Bardow, A.; Kreutzer, M. T. *Lab Chip* **2012**, *12*, 3387–3391.
- (19) Liu, N.; Aymonier, C.; Lecoutre, C.; Garrabos, Y.; Marre, S. *Chem. Phys. Lett.* **2012**, *551*, 139–143.
- (20) Abolhasani, M.; Kumacheva, E.; Günther, A. *Ind. Eng. Chem. Res.* **2015**, *54*, 9046–9051.
- (21) Abolhasani, M.; Günther, A.; Kumacheva, E. *Angew. Chem., Int. Ed.* **2014**, *53*, 7992–8002.
- (22) Marine, N. A.; Klein, S. A.; Posner, J. D. *Anal. Chem.* **2009**, *81*, 1471–1476.
- (23) Wattanasin, P.; Saetear, P.; Wilairat, P.; Nacapricha, D.; Teerasong, S. *Anal. Chim. Acta* **2015**, *860*, 1–7.
- (24) Poulsen, C. E.; Wootton, R. C. R.; Wolff, A.; deMello, A. J.; Elvira, K. S. *Anal. Chem.* **2015**, *87*, 6265–6270.
- (25) Alimuddin, M.; Grant, D.; Bulloch, D.; Lee, N.; Peacock, M.; Dahl, R. J. *Med. Chem.* **2008**, *51*, 5140–5142.
- (26) Abolhasani, M.; Bruno, N. C.; Jensen, K. F. *Chem. Commun.* **2015**, *51*, 8916–8919.
- (27) Abolhasani, M.; Oskoei, A.; Klinkova, A.; Kumacheva, E.; Gunther, A. *Lab Chip* **2014**, *14*, 2309–2318.
- (28) Gielen, F.; van Vliet, L.; Koprowski, B. T.; Devenish, S. R. A.; Fischlechner, M.; Edel, J. B.; Niu, X.; deMello, A. J.; Hollfelder, F. *Anal. Chem.* **2013**, *85*, 4761–4769.
- (29) Abolhasani, M.; Coley, C. W.; Xie, L.; Chen, O.; Bawendi, M. G.; Jensen, K. F. *Chem. Mater.* **2015**, *27*, 6131–6138.
- (30) Bico, J.; Quéré, D. *J. Fluid Mech.* **2002**, *467*, 101–127.
- (31) Chen, D. L.; Li, L.; Reyes, S.; Adamson, D. N.; Ismagilov, R. F. *Langmuir* **2007**, *23*, 2255–2260.
- (32) Banerjee, S.; Verma, P.; Mitra, R.; Basu, G.; Pal, S. *J. Fluoresc.* **2012**, *22*, 753–769.
- (33) Hansch, C.; Leo, A. *Exploring QSAR*; American Chemical Society: Washington, DC, 1995.